

# DarcyTools: A Computer Code for Hydrogeological Analysis of Nuclear Waste Repositories in Fractured Rock

Urban Svensson<sup>1</sup>, Michel Ferry<sup>2</sup>

<sup>1</sup>Computer-aided Fluid Engineering AB, Frankes väg 3, 371 65 Lyckeby, Sweden

<sup>2</sup>MFRDC, 6 rue de la Perche, 44700 Orvault, France

Email: [us@cfe.se](mailto:us@cfe.se), [mf@mfrdc.com](mailto:mf@mfrdc.com)

Received January 2014

---

## Abstract

A computer code for simulation of groundwater flow and transport is described. Both porous and fractured media are handled by the code. The main intended application is the analysis of a deep repository for nuclear waste and for this reason flow and transport in a sparsely fractured rock is in focus. The mathematical and numerical models are described in some detail. In short, one may say that the code is based on the traditional conservation and state laws, but also embodies a number of submodels (subgrid processes, permafrost, etc). An unstructured Cartesian grid and a finite volume approach are the key elements in the discretization of the basic equations. A multi-grid solver is part of the code as well as a parallelization option based on the SPMD (Single-Program Multiple-Data) method. The main application areas are summarized and an application to a deep repository is discussed in some more detail.

## Keywords

Fractured Rock, Inflow Prediction, Deep Repository

---

## 1. Introduction

### 1.1. Background

DarcyTools is a computer code for simulation of flow and transport in porous and/or fractured media. The fractured media in mind is a fractured rock and the porous media is the soil cover on the top of the rock; it is hence groundwater flow, which is the class of flows in mind. The code is intended to be applicable to a wide range of groundwater flows, but the analysis of a repository for nuclear waste is the main intended application. For the present purposes, the repository can be defined as a set of tunnels and holes for deposition of canisters. It is further expected that the repository will be placed at a depth of about 500 metre, in a sparsely fractured rock.

Flow and transport in a sparsely fractured rock is due to a system of fractures and faults, spanning scales from mm to km. A groundwater model should hence represent this network of fractures and then simulate the flow and transport in the network.

Two basic approaches in groundwater modelling can be identified; in one, grid cell conductivities are defined (sometimes called the continuum porous-medium (CPM) approach, e.g. [1]), while in the other, the flow through the network is calculated directly (discrete fracture network (DFN) approach). Both approaches have their merits and drawbacks, though these will not be discussed in this paper (for discussions, see e.g. [2] [3]). DarcyTools is based on a method that combines the approaches, meaning that a fracture network is first generated and then the network is represented as grid cell conductivities. The resulting property fields are expected to have some desirable features, such as realistic correlation and anisotropy structure, provided the network is properly represented in the grid.

DarcyTools uses an unstructured Cartesian grid, that allows for local refinements around tunnels, boreholes, fracture zones, etc. After the equations have been discretized, using a finite volume approach, the resulting system of equations is solved by a multigrid solver. For a detailed description of the code and its use, the reader is referred to three reports that give a full account of the code ([4]-[6]).

A number of well-established codes for repository analysis are available: TOUGH2 [7], MODFLOW [8], PFLTRAN [9], Connect Flow [3] and FRACMAN [10] to mention a few. In order to relate DarcyTools to these codes some strong points and limitations of DarcyTools are listed.

Strong points:

- A fracture network, built on both deterministic and random fractures, is easily generated or imported from another fracture generator. Sub grid fractures are considered by a sub grid model.
- An unstructured grid resolves objects (repository, lakes, fracture zones, etc) read in as CAD files. Computational cells can be removed or refined according to various criteria.
- Efficient numerical solutions; multigrid techniques, parallelization, etc.

Limitations:

- Chemical reactions and multiphase flow are not simulated by DarcyTools.
- Thermo-hydro mechanical effects [11] are not handled in the present version of DarcyTools.

## 1.2. Objective

The main objective is to describe the computer code DarcyTools. The scope, features, basic equations, numerical methods and an application to a deep repository case will be briefly described.

## 2. Scope

### 2.1. Introduction

Simulations for the analysis of a nuclear waste repository are, as stated, the main intended application. This, however consists of a broad range of simulations, both with respect to space and time scales. Simulations of the flow below inland ice sheets (relevant in long term scenario studies of a repository) with very large space and time scales may be considered, contrasted with transport at the interface between a deposition hole and the rock (flow and diffusion on the mm scale). In this section, the scope will be illustrated by a discussion of the processes on scales ranging from the 10 km scale down to the mm scale.

### 2.2. The 10 km Scale View

The regional groundwater flow in unconfined aquifers introduces the concepts of recharge and discharge areas, see **Figure 1**. Recharge areas, *i.e.* where a net inflow is found, are usually found in topographically high places while the discharge areas are located in topographic lows. A discharge area may take the form of a stream, river or a lake.

The general flow pattern is thus from high to low areas; a system of local flow cells is formed and the groundwater table follows the surface topography. However, this is an idealized picture based on the assumptions of a steady and constant density flow in a homogeneous aquifer. These assumptions are seldom fulfilled and care should hence be taken when interpreting field data. In particular, most natural aquifers are anisotropic and heterogeneous.

### 2.3. The km Scale View

A km scale view is provided in **Figure 1**. Let us assume that it is of interest to determine the origin of water

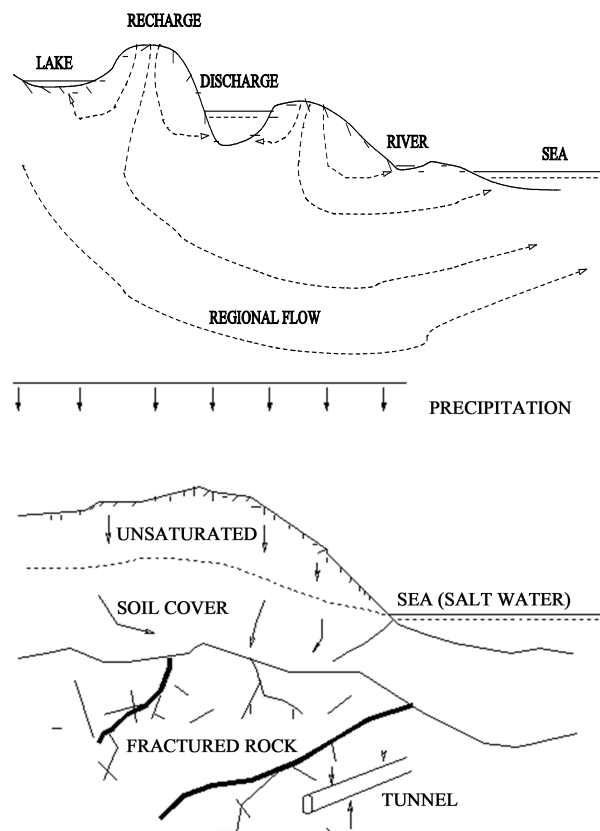


**Figure 1.** Situations considered. The 10 km scale view (top) and the km scale view.

leaking into a tunnel. Two main sources of water are precipitation and sea water (excluding brine water from below). To track the precipitation water it is needed to follow a water parcel through the unsaturated zone, through the saturated soil cover and finally its way through the fracture network. It is essential to determine the position of the groundwater table, as it determines the pressure gradients in the porous medium and may influence the conditions deep in the rock. The other source, the sea water, introduces density effects, as the seawater has higher density than fresh water. The heavier saltwater penetrates the coastal zone and modifies the pressure distribution (the Ghübern Herzberg relation). Due to this effect the inflow into the tunnel may be dominated by sea water or precipitation water depending on the actual conditions (density difference, tunnel position, etc).

## 2.4. The m Scale View

The main novel features of DarcyTools are concerned with the fracture network and focus will therefore be on the description of fractures (giving the porous media less attention). In **Figure 2** part of a fracture network is shown. Different parts of the network have been marked with letters; these parts will now be described:

**A:** Represents a fracture zone. The fracture zone is assumed to be composed of a number of smaller fractures through which the flow takes place. However, most of the small fractures do not contribute to the flow but are important nonetheless for transport and dispersion of a tracer. Fracture zones are often the main flow conductors due to their high transmissivity and size (length scale >100 metres). The typical thickness is >1 metre.

**B:** Some fractures are best characterized as “a single opening”. The typical thickness, or the aperture, is on the order of  $10^{-3}$  metres. The fractures marked with **B** in **Figure 2** have a through-flow and may thus contribute to the total flow rate. If the transport time through the **B** fractures is different from the transport time in the fracture zone, a dispersion effect will also result from the parallel flow path.

**C:** Isolated fractures, or groups of isolated fractures, cannot contribute to the flow, transport or dispersion, as flow in the matrix is normally neglected. In the numerical model these are removed prior to grid data generation.

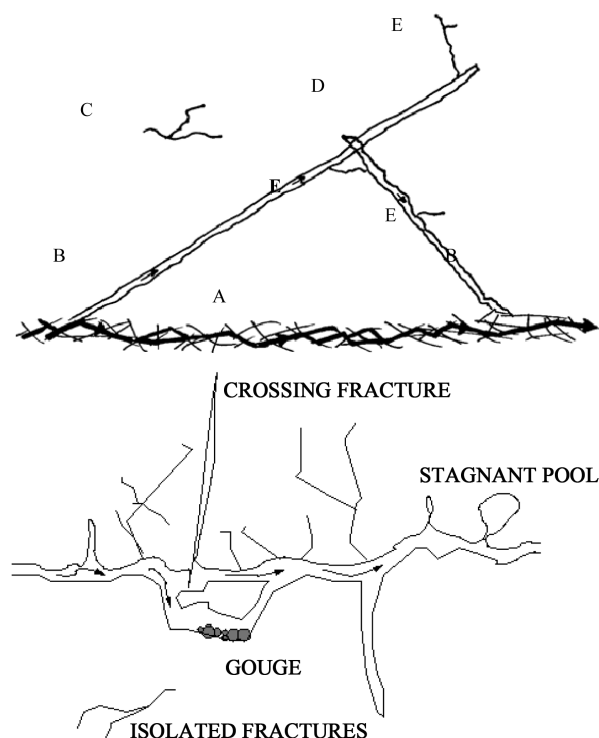


**Figure 2.** Situations considered. The m scale view (top) and the mm scale view.

**D:** Some fractures, or fracture zones, may form “dead end systems”. The exchange with fractures with significant flows is then by molecular diffusion. When solute transport or storage of water over long time periods, say longer than 100 years, is studied it is essential to represent the dead-end systems correctly.

**E, F:** There is always a lower limit on the fracture size that can be correctly represented in a numerical simulation. In the present formulation, it will be assumed that fractures below a certain size do not contribute significantly to the total flow. However, for transport and dispersion it is probably necessary to consider all scales, as a large fraction of the pore volume is expected to be due to the small scale features of the fracture network.

### 2.5. The mm Scale View

It was mentioned above that the opening, or aperture, of a fracture is typically on the order of 1 mm or smaller. However, the aperture does not have a constant value, as is illustrated in **Figure 2**. On this scale, it is useful to introduce the notions of the mobile zone for the volume that has flowing water and the immobile zone, which represents all volumes with stagnant water. In **Figure 2**, the stagnant pools, the crossing fractures and the matrix may all contain stagnant water. The fracture may also contain geological material of various kinds, so called gouge material.

It is essential to consider the geometrical complexity of a fracture opening when describing small scale dispersion processes. The exchange between the mobile and immobile zones is often assumed to be due to molecular diffusion only.

## 3. Main Features

The main features of DarcyTools are summarized in **Table 1**. In short, one may say that a fracture network is represented on an unstructured Cartesian grid and the resulting finite volume equations are solved by a multigrid solver. An elaboration of some of the features listed in **Table 1** follows below:

- Fracture network. Deterministic fractures and fracture zones are assumed to be known with respect to position and extent. Other properties, such as transmissivity, may also have been evaluated from field tests. Random fracture sets are generated with a power law for size distribution and a Fisher distribution for orient-

**Table 1.** Main features.

Feature	Description
Fracture network	Network with deterministic and random fractures. Fisher distribution for orientation. Heterogeneous fractures.
Matrix exchange	A multi-rate, or single rate, diffusion concept. Handles both particles and advection/diffusion equations.
Free groundwater surface	An algorithm that focuses on the position of the groundwater table.
Particle tracking	Two options, traditional flow following and a cell-jump method.
Tunnels and boreholes	Introduced as CAD-objects. Routines for setting pressure and grouting conditions.
Water type analysis	A series of advection/diffusion equations are solved to track waters of different origin (in space and time).
Gravitational effects, buoyancy	Full coupling through the density laws with salinity and temperature fields.
Basic equations	Darcy's law. Conservation equations. State laws for properties.
Grid system	Unstructured Cartesian grid.
Representation of fractures on the grid	Cell properties calculated according to the intersecting volumes between fractures and cells.
Discretization method	Finite volumes. Hybrid schemes.
Solver, parallelization	Multigrid solver. SPMD (Single Program Multiple Data) parallelization.

tation. Normally a Poisson distribution is used for spatial positions. Random fractures, or groups of fractures, may be removed if isolated. A limited number of deterministic fractures can be given heterogeneous properties (in order to achieve channelling effects for flow).

- Matrix exchange. Fractures that cannot be explicitly represented in the computational grid are handled by a subgrid model. This model is based on the multi-rate diffusion model [12] and an assumption of a power law for fracture size distribution. The subgrid model is implemented both for advection/diffusion equations, for example used for salinity, and for a particle tracking routine. A single-rate option for simulating a matrix with uniform properties is also implemented.
- Free groundwater surface. The free surface algorithm focuses on the position of the groundwater table. The position is determined by the local mass balance, but does not consider the properties of the unsaturated zone.
- Tunnels and boreholes. The grid generator reads the CAD files for these objects and refines the grid locally around the objects according to various criteria. Grouting around tunnels can be simulated by putting conditions on the hydraulic conductivity in layers around the tunnel. Various boundary conditions (fixed inflow, fixed pressure, etc) can be associated with the objects.
- Representation of fractures on the grid. The basic technique is described in detail in [13] and [14]. In these papers it is shown that the method is accurate and effective.

## 4. Mathematical Formulation

### 4.1. Introduction

The mathematical formulation is straightforward as the conservation and state laws are formulated in a fairly standard way.

### 4.2. Conservation Laws

Conservation of mass:

$$\frac{\partial \rho \theta}{\partial t} + \frac{\partial}{\partial x}(\rho u) + \frac{\partial}{\partial y}(\rho v) + \frac{\partial}{\partial z}(\rho w) = Q \quad (1)$$

where  $\rho$  is fluid density  $\theta$ , porosity,  $u$ ,  $v$  and  $w$  Darcy velocities and  $Q$  a source/sink term. The coordinate

system is denoted  $x, y, z$  (space) and  $t$  (time).

Mass fraction transport equation:

$$\frac{\partial \rho \theta C}{\partial t} + \frac{\partial}{\partial x} \left( \rho u C - \rho \gamma D_x \frac{\partial C}{\partial x} \right) + \frac{\partial}{\partial y} \left( \rho v C - \rho \gamma D_y \frac{\partial C}{\partial y} \right) + \frac{\partial}{\partial z} \left( \rho w C - \rho \gamma D_z \frac{\partial C}{\partial z} \right) = Q C + Q_c \quad (2)$$

where  $C$  is transported mass fraction,  $D_x, D_y$  and  $D_z$  the normal terms of the diffusion-dispersion tensor and  $Q_c$  a source/sink term, that represents the exchange with immobile zones. Note that the diffusion coefficients are the effective coefficients that include the porosity, see further explanation of the diffusion term in connection with Equation (11) below.

Conservation of heat:

$$\frac{\partial (\rho \theta c_p + (1-\theta)c)T}{\partial t} + \frac{\partial}{\partial x} \left( \rho u c_p T - \lambda_x \frac{\partial T}{\partial x} \right) + \frac{\partial}{\partial y} \left( \rho v c_p T - \lambda_y \frac{\partial T}{\partial y} \right) + \frac{\partial}{\partial z} \left( \rho w c_p T - \lambda_z \frac{\partial T}{\partial z} \right) = Q c_p T + Q_T \quad (3)$$

where  $\lambda_x, \lambda_y$  and  $\lambda_z$  are the normal terms of the equivalent (*i.e.* rock with fluid) thermal conductivity tensor,  $c$  is the rock thermal capacity and  $c_p$  the specific heat of the fluid and  $Q_T$  a source/sink term. We are hence only solving for one temperature, assuming thermal equilibrium between the rock and the water. Note that we have chosen to use  $c$  (Joule/m<sup>3</sup> °C) for the rock thermal capacity and  $c_p$  (Joule/kg °C) for the specific heat of the fluid. The reason for this inconsistency is that this formulation does not require the rock density as an input variable.

The mass conservation equation is turned into a pressure equation under the well-known Darcy's law:

$$\begin{aligned} \rho u &= -\frac{K_x}{g} \frac{\partial P}{\partial x} \\ \rho v &= -\frac{K_y}{g} \frac{\partial P}{\partial y} \\ \rho w &= -\frac{K_z}{g} \frac{\partial P}{\partial z} - K_z (\rho - \rho_0) \end{aligned} \quad (4)$$

where  $K_x, K_y$  and  $K_z$  are the local hydraulic conductivities in  $x, y$  and  $z$  direction,  $g$  the gravity acceleration,  $\rho_0$  a reference fluid density and  $P$  the dynamic fluid pressure relative to the reference hydrostatic pressure

$$P = p + \rho_0 g z \quad (5)$$

where  $p$  is the total pressure. The hydraulic conductivity,  $K$ , is related to the permeability,  $k$ , by the relation:

$$K = \frac{\rho g k}{\mu} \quad (6)$$

where  $\mu$  is the dynamic viscosity.

### 4.3. State Laws

The fluid properties like the dynamic viscosity,  $\mu$ , the density,  $\rho$ , and the specific heat,  $c_p$ , are given by state laws:

$$\mu = \mu_0 \left[ 1 + a_1 (T - T_\mu) + a_2 (T - T_\mu)^2 \right]^{n_\mu} \quad (7)$$

$$\rho = \rho_0 \left[ 1 + \alpha_1 S + \alpha_2 S^2 - \beta_1 (T - T_\rho) - \beta_2 (T - T_\rho)^2 \right] \quad (8)$$

$$c_p = c_{p0} (1 + b_1 S + b_2 S^2) \quad (9)$$

while the porosity  $\theta$  and the compaction,  $\gamma$ , of the matrix are given the following dependencies:

$$\theta = \theta_0 \gamma \quad (10)$$

$$\gamma = 1 + (\sigma/\theta_0) (P - P_0)/\rho g \quad (11)$$

In the above formulas  $S$  represents the salinity (salt mass fraction),  $\theta_0$  a reference porosity field given for a reference pressure field  $P_0$  and  $\sigma$  the specific storativity field.  $n_\mu$ ,  $a_i$ ,  $b_i$ ,  $\alpha_i$ ,  $\beta_i$ ,  $\mu_0$ ,  $\rho_0$ ,  $c_{p0}$ ,  $T_\mu$  and  $T_\rho$  are constants. Equations (7) to (9) thus provide linear and quadratic dependencies of salinity and temperature. It is the user's task to find the best coefficients for a given problem.

In the advection/diffusion Equation (2), it is common to write the diffusion coefficient as  $\theta D_{mol}$ , where  $D_{mol}$  is the molecular diffusion coefficient. In DarcyTools we choose to write the term as  $\theta D_{mol} = \theta_0 \gamma D_{mol} = \gamma D$ , where  $D$  is now the effective diffusion coefficient.

#### 4.4. Additional Models

DarcyTools embodies a number of additional special purpose models. The most important of these are:

- Subgrid model. When the transport of a substance (salt, radionuclide, etc.) is to be analyzed, it is necessary to consider processes on the mm scale, see **Figure 2**. A number of processes, on a range of time and space scales, contribute to the dispersion of a substance as it travels with the flow. The processes on the mm scale are often very significant and DarcyTools includes a sub grid model [12], to deal with these processes.
- Permafrost model. DarcyTools contains a model to simulate the permafrost freezing and thawing process. To take into account the phase change of water when the temperature goes below the melting-point, the source terms of Equations (1), (2) and (3) are modified. Properties such as permeability or thermal conductivity are also highly dependent on the ice content.
- Grouting model. As mentioned in Section 3, the hydraulic conductivity in the near field of a tunnel can be modified, in order to simulate the effect of grouting.

### 5. Numerical Methods

#### 5.1. Introduction

The conservation laws are represented on a computational grid using the finite volume method. The finite volume method integrates equations over the faces of a finite number of control volumes by converting volume integrals into surface integrals using the Ostrogradsky and the mean value theorems:

$$\int_V \text{div}(\vec{F}) dV = \int_{\partial V} \vec{F} \cdot \vec{n} dA = \sum_{i=1}^{nbfaces} A_i \vec{F}_i \cdot \vec{n}_i \quad (12)$$

where,  $A_i$  and  $n_i$  are respectively the area and the outside-normal of the cell face named  $i$  and where the flux value  $F_i$  is evaluated at face centre.

#### 5.2. Discretization in Space

Among the common grid arrangements, DarcyTools uses the “cell-centred” arrangement [15] in which the pressure and the scalar variables (mass fractions) are located at centre of grid cells, see **Figure 3** and **Figure 4**. The

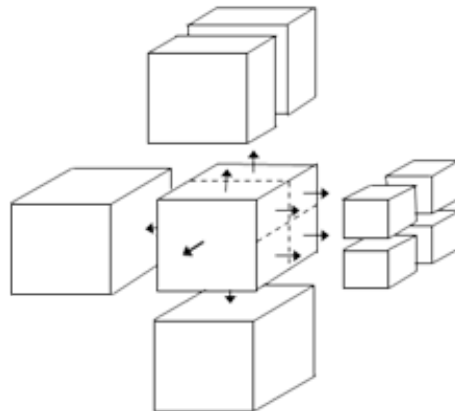


**Figure 3.** Unstructured Cartesian control volumes, faces and normals.

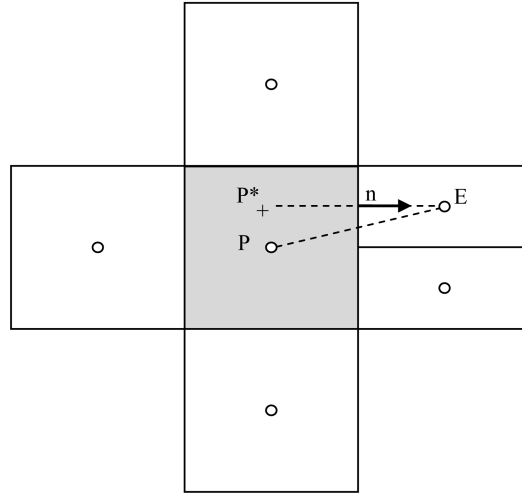


**Figure 4.** Cell-centred arrangement labelling.

main advantage of this formulation is the fact that control volumes coincide with grid cells and that cell vertices are directly defined by grid nodes. The main drawback is the fact that, for non-uniform meshes, the faces of control volumes may not be located mid-way between variable locations or may not be orthogonal to the line joining cell centers. More sophisticated interpolations are therefore necessary to get a second order discretization of convective and diffusive fluxes.

For stability reasons the discretization in space of Equations (1), (2) and (3) involves both convective and diffusive fluxes according to the Hybrid Differencing Scheme [16]. This scheme (13) is based on a combination of central and upwind differencing schemes depending on the value of the local Peclet number. For Peclet numbers smaller than two the scheme is second order while for higher Peclet numbers it is only accurate to first order but accounts for transportiveness [17]

$$F_i = \left( c \phi - d \frac{\partial \phi}{\partial x} \right)_i = a \phi_{P^*} + (c - a) \phi_E \quad (13)$$

$$a = \max \left( 0, c, \frac{h^+ c + 2d}{h^+ + h^-} \right) \quad (14)$$

$$\phi_{P^*} = \phi_P + \left( \overline{PE} - (\overline{PE} \bar{n}) \bar{n} \right) \overline{grad} \phi_P \quad (15)$$

where  $h^+$  and  $h^-$  represent respectively the size of cell  $E$  and cell  $P$  and where the cell centred gradient is given by the Gauss theorem as:

$$\overline{grad} \phi = \frac{1}{V} \sum_{i=1}^{nbfaces} A_i \phi_i \bar{n}_i \quad (16)$$

where  $V$  represents the volume of the cell and  $\phi_i$  the face value of the quantity under consideration.

$$\phi_i = \frac{h^+}{h^+ + h^-} \phi_{P^*} + \frac{h^-}{h^+ + h^-} \phi_E \quad (17)$$

Since in Equation (16) the face values (17) are linked to the gradient through (15), the gradient value is obtained after some iterations of a fix point algorithm. Three iterations produce a sufficient accuracy for most uses.

### 5.3. Time Discretization

To ensure the precision of time dependent simulations, when users specify transient boundary conditions and time variations of time steps, DarcyTools discretizes the time derivative term of Equations (1), (2) and (3) as a fully implicit second order backward finite difference:

$$\left. \frac{\partial \phi}{\partial t} \right|_n = \frac{2\Delta t_1 + \Delta t_2}{\Delta t_1(\Delta t_1 + \Delta t_2)} \phi_n - \frac{\Delta t_1 + \Delta t_2}{\Delta t_1 \Delta t_2} \phi_{n-1} + \frac{\Delta t_1}{\Delta t_2(\Delta t_1 + \Delta t_2)} \phi_{n-2} \quad (18)$$

where  $\Delta t_1$  and  $\Delta t_2$  represent respectively the time steps  $t_n - t_{n-1}$  and  $t_{n-1} - t_{n-2}$ . However, a first-order backward implicit Euler scheme, less demanding in memory, is also possible for simply relaxing non-linear steady flow simulations:

$$\left. \frac{\partial \phi}{\partial t} \right|_n = \frac{\phi_n - \phi_{n-1}}{t_n - t_{n-1}} \quad (19)$$

#### 5.4. Cartesian Grids

With structured grids, local refinements may drastically increase the total number of cells by propagating cell size reductions up to boundaries, see **Figure 5**. To avoid this generation of useless cells in regions of low interest, DarcyTools uses adaptive Cartesian grids [18]. Starting with a single cell that covers the entire domain, the grid generator successively splits cells requiring refinement in two half children cells and repeats this procedure for each direction until the cell size, or the total number of cells, reaches threshold values.

These threshold values as well as cell removal criteria are user defined during the initial grid construction but also during any grid update according to rock properties. Zones with different cell sizes, or cell removal criteria, may be defined from predefined objects such as lines, planes, parallelepipeds, cylinders or spheres, but mainly from real triangulated shapes stored from CAD software using the STL (Stereo Lithography) file format.

Though cell information could be stored in an octree data structure, DarcyTools implements a fully unstructured data structure where cell locations and sizes are stored in a compact structure using only fifteen bytes per cell.

#### 5.5. Solver

DarcyTools uses a GMRES Krylov subspace solver [19] in association with a multigrid preconditioner [20] to achieve a fast and robust convergence of the algebraic sets of equations resulting from successive discretizations. To simultaneously adapt its coarse grid operators to the unstructured Cartesian grid and to the rock properties, the multigrid preconditioner in use is based on an algebraic multigrid method [21] which uses only the information available in the linear system of equations.

The multigrid method improves the reduction of long wave length error components, which is important for solving the mass conservation equation with iterative methods. The GMRES method ensures the robustness of the solver when sharp variations of physical properties in the fractured rock ill-condition the algebraic sets of equations for the Incomplete Lower-Upper factorization (ILU0) smoother.

When the buoyancy term of Equation (4) slows down the convergence, because of the non-linear coupling between the mass conservation equation and the salt transport equation, DarcyTools uses one of the capabilities of its multigrid preconditioner [22] which consists in simultaneously iterating both equations in a strongly coupled manner in order to accelerate the global convergence.

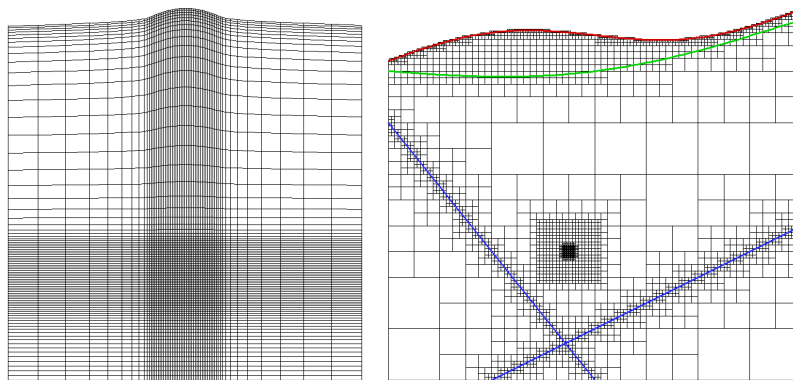


**Figure 5.** Structured vs unstructured grids.

## 5.6. Parallelization

The parallelization techniques employed in DarcyTools rely on a Single-Program Multiple-Data (SPMD) approach which consists in first partitioning the grid and then in executing the same piece of code repeatedly on each block.

By default, DarcyTools automatically partitions the domain using a Hilbert space-filling curves technique, taking advantage of the Cartesian structure of the grid [23] and [24]. Given a list of cells in the original domain, a space-filling curve is built that passes through each cell once, see **Figure 6**. The map is constructed so that cells that are close in 3D space remain close when mapped. Thus, the curve preserves locality. Once the curve is constructed, the decomposition of the domain is performed by dividing it into  $N$  subintervals, where  $N$  is the number of processors to be used. For load balancing the length of any subinterval can be specified in term of percentage of the total length. When load balance is crucial, users may specify their own partition.

To avoid scalability limitations due to memory bandwidth, and to enable runs on distributed memory clusters, DarcyTools implements the Message-Passing-Interface (MPI) technique for communication between the blocks of the domain. This choice does not restrict the applicability of DarcyTools to clusters since the same MPI technique equally applies on multi-core shared memory computers.

## 6. Application Areas

Even if a wide range of groundwater flow problems can be simulated with DarcyTools, most applications have so far been related to the analysis of a nuclear waste repository. The Forsmark site (located around 120 km north of Stockholm, Sweden) is of particular significance as the Swedish Nuclear Fuel and Waste Management Company (SKB) has submitted a license application for the construction of a final repository at this site. An introduction to the Forsmark site, and the modelling tasks carried out, is given by [25]. For the present objectives we show a map over the area, see **Figure 7**, and note that it is a coastal site with a number of small shallow lakes. The application areas are summarized in **Table 2** and an elaboration is given by the following points:

- Site investigations. At Forsmark, the water in the bedrock is saline with a salinity that increases with depth. The resulting density field will influence the undisturbed flow pattern and it is hence of interest to simulate and understand the present day salinity distribution. Simulations covering a period of about 10,000 years (since the last glaciation) have been carried out considering the variation in water level and salinity of the Baltic Sea during the period.
- Open repository. The open phase of a repository is expected to be around 50 years and during this time interval different parts of the repository will be opened and closed successively. It is of interest to know the inflow distribution, in space and time, during this phase as the inflow is related to effects like drawdowns of the groundwater table and upconing of salt water from below the repository. One way to control the inflow rate is by grouting, a process that also needs to be simulated in order to estimate the reduction of the inflow. The open phase of the Forsmark repository will be discussed in more detail in the next section.

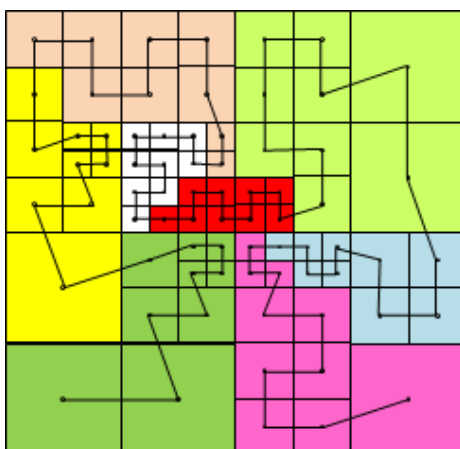


**Figure 6.** Example of Paneo-Hilbert space-filling curve partitioning.

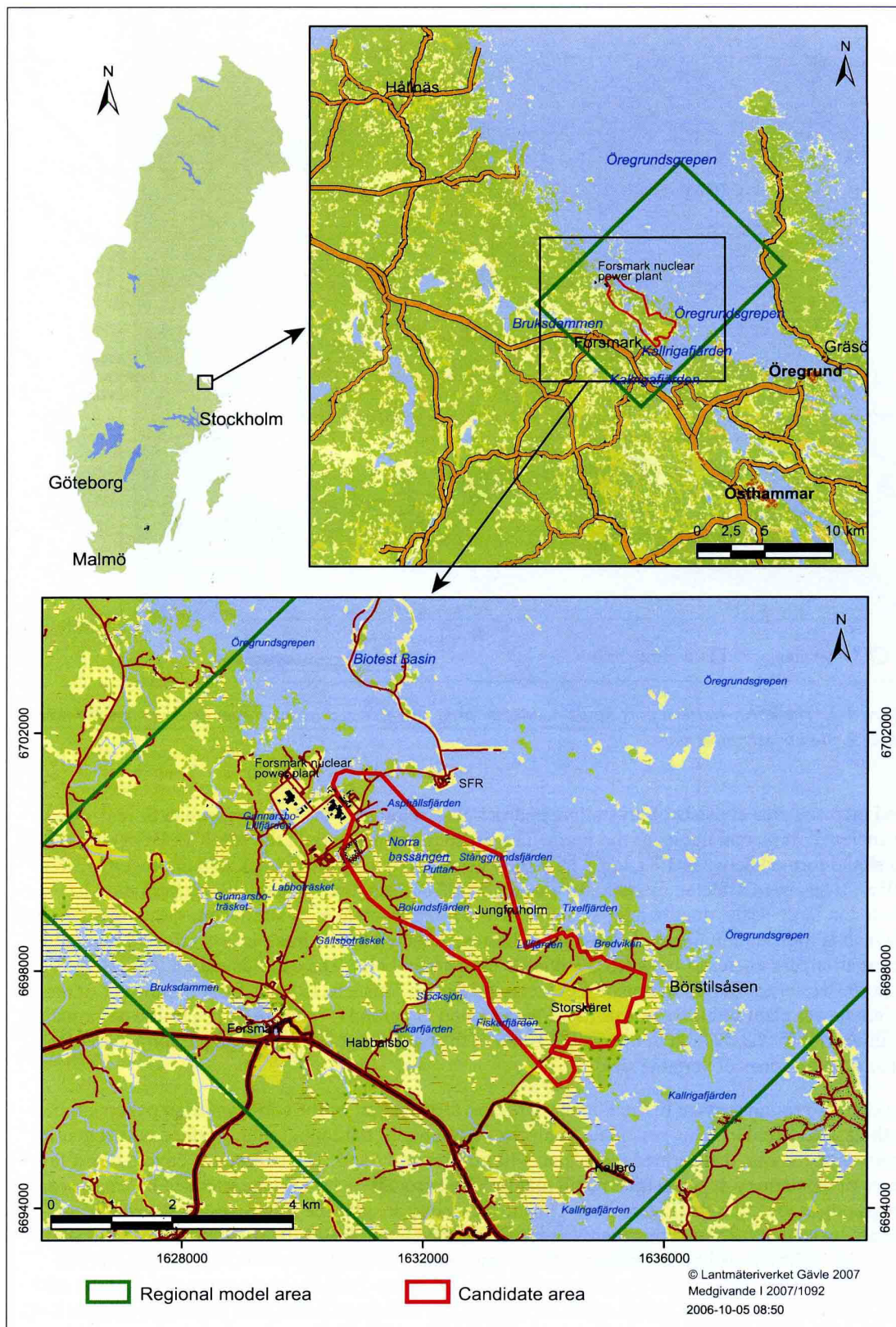


**Figure 7.** The red polygon shows the size and location of the candidate area for site investigations at Forsmark. The green rectangle indicates the size and location of the regional model area used in the analysis of the site.

**Table 2.** Key application areas.

Application	Description
Site Investigation	Development of salinity field since last glaciation. Natural flow system. Water type evolution. Super regional models. Borehole analysis.
Open repository	Inflow distribution in space and time. Draw downs. Resaturation of backfill. Grouting.
Permafrost and Glaciation	Long term scenarios. Ice sheets.
Surface hydrology	Surface waters and their interaction with the groundwater system. Transport in lakes, streams and near ground.
Transport and retention	Transport of radionuclides from a deposition hole to ground surface. Reactive transport.

- Transport and retention. After closure of the repository there will be a stage during which the tunnel backfill and the bentonite clay enclosing the canisters are saturated. After this stage a flow pattern that is close to the undisturbed situation can be expected. The whole transport path, from the canister, through the fracture network and through the lakes and streams then needs to be analyzed. Close to the canisters matrix diffusion may be the dominating mode of transport.
- Surface hydrology. In the performance and safety assessment of a repository, it is of interest to include the surface water system (lakes and streams) for at least two reasons: 1) During the operational phase one can expect a drawdown of the groundwater table, due to the inflow to the open repository. This drawdown needs to be estimated due to its environmental impact. 2) Lakes and streams provide a link in the transport chain from a deposition hole to the sea. All parts of the possible transport paths are essential to understand.
- Permafrost and Glaciation. The objective of these studies is to provide bounding hydrogeological estimates at different stages during glaciation and deglaciation of a glacial cycle [26].

## 7. The Open Phase of the Forsmark Repository

### 7.1. Introduction

The main objective of the modelling of the open phase is to evaluate the hydrogeological effects caused by an open repository. In particular, the following is studied:

- the magnitude and spatial distribution of the inflow to the open repository,
- the magnitude and spatial distribution of the drawdown of the groundwater table,
- the chemical composition (*i.e.* salinity) and spatial distribution of the groundwater in proximity of the open repository,
- the role of grouting for the inflow, drawdown and upconing phenomena, and
- the saturation period after the open repository has been closed (backfilled).

The mathematical modelling of the repository considers three operation stages, A-C (see **Figure 8**), which were run in sequence, where the first stage, stage A, lasted for 15 years, stage B lasted for 15 years and stage C lasted for 20 years. Hence, the total operation time was 50 years. The role of grouting was looked at by modelling three levels of grouting efficiency, I-III, see **Table 3**. A full account of this work can be found in [27]; here we will focus on the set-up of the computational grid and some results concerning inflow to the repository.

### 7.2. Set-Ups

The computational grid was refined in the vicinity of the repository in order to resolve the repository layout and to study the effects of grouting. The largest cell size away from the repository was 128 metres (**Figures 9-11**) and in the proximity of the repository the cell size was 4 metres. This high resolution was needed to resolve the deposition tunnels, which have a height of 4.8 metres and width of 4.2 metres. A vertical cross-section through the repository is shown in **Figure 12**; the vertical resolution of the cells close to the top boundary was 2 metres. In total about 1.4 million cells were used to model the problem as outlined.

The geometry and hydraulic properties of discrete geological features in the bedrock such as deformation zones, sheet joints and fracture network realizations were imported from the work by [28]. The vertical permeability field around the repository, as represented on the grid, is shown in **Figure 13**.

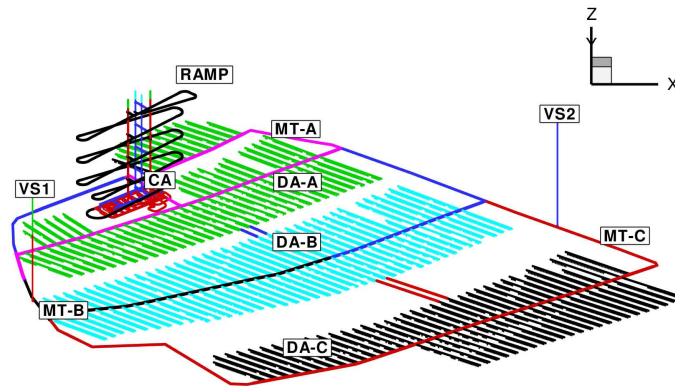


**Figure 8.** Definition of different parts of the studied repository layout at Forsmark. The mathematical modelling considers three operation stages, A-C, and three possible grouting levels for each stage. The three stages are indicated by green, turquoise and pink colours. DA = deposition area, MT = transportation and main tunnel, VS = ventilation shaft, CA = central area. The deposition tunnels are shown as branches to the main tunnels and the canister holes (almost invisible) are drilled from the bottom of the deposition tunnels.

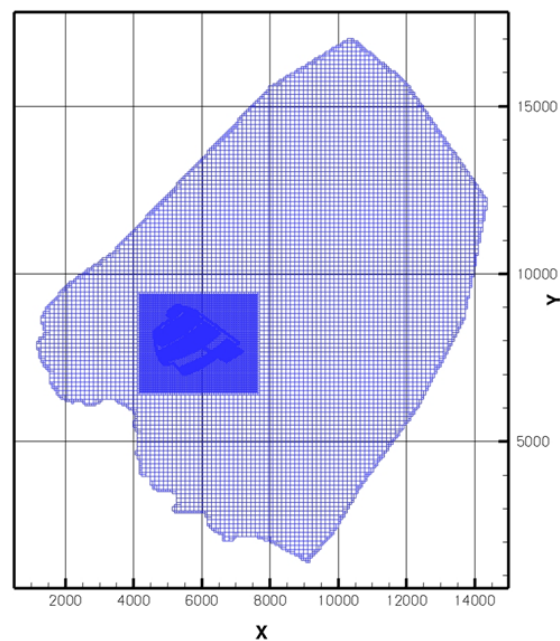


**Figure 9.** Plan view of the model area and the computational grid at -465 m elevation. The size of the largest grid cells is 128 m.

**Table 3.** Definition of the studied levels of grouting efficiency.

Level	Definition
I	The hydraulic conductivity of all cells in contact with the repository has a maximum value of $1 \times 10^{-7}$ m/s.
II	The hydraulic conductivity of all cells in contact with the repository has a maximum value of $1 \times 10^{-8}$ m/s.
III	The hydraulic conductivity of all cells in contact with the repository has a maximum value of $1 \times 10^{-9}$ m/s except where the modelled ungrouted hydraulic conductivity is $10^{-6}$ m/s or greater. At these positions the hydraulic conductivity has a maximum value of $1 \times 10^{-8}$ m/s.

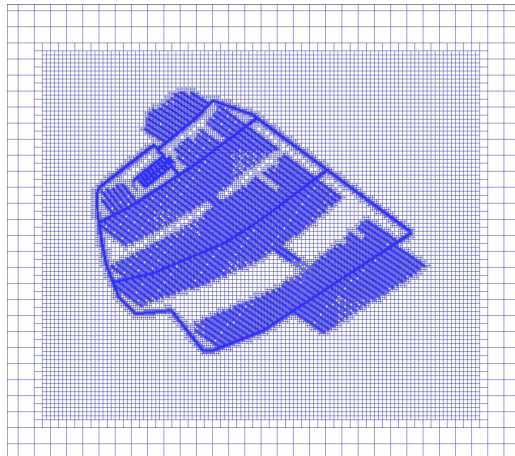


**Figure 10.** Plan view of the computational grid at -465 m elevation. The discretisation around the repository was refined using an unstructured grid.

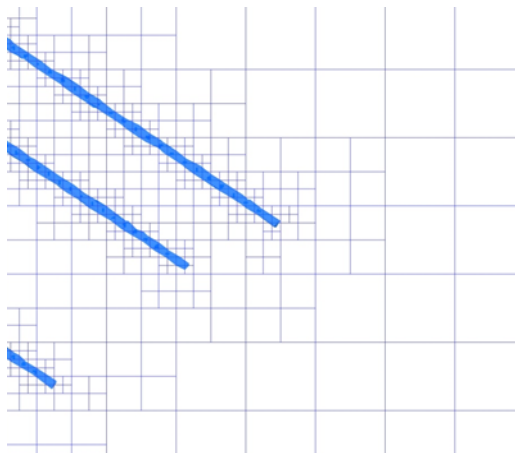


**Figure 11.** Enlargement showing the discretisation of the eastern corner of the repository. The size of the smallest grid cells is 4 m.

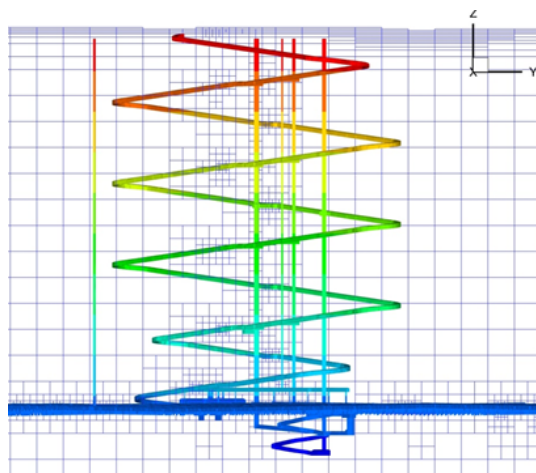


**Figure 12.** Vertical cross-section (South-North) through the simulated repository. The y-axis points towards north.

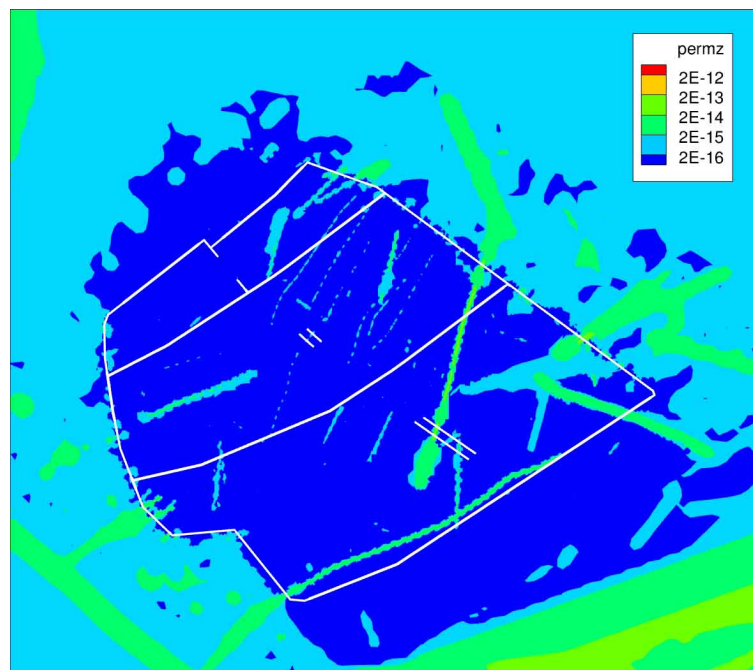


**Figure 13.** Plan view of the grid cell vertical permeability field in the target area at  $-465$  m elevation. The white lines represent the main tunnels.

### 7.3. Flow Simulations

The inflow simulations during the excavation and operation phases were done in a transient mode for the three operation stages A-C (**Figure 8**) and three levels of grouting efficiency I-III (**Table 3**). **Table 4** summarizes the calculated inflows to the different parts of the repository. The total inflow varied in the range of 7 to 52 L/s (600 to 4600 m<sup>3</sup>/d), depending on which stage and level of grouting efficiency that is considered.

An illustration of the inflow distribution is given by **Figure 14**, which represents operation stage C, *i.e.*, the last one of the three operation stages and grouting level II. Operation stage C rendered the largest inflows. For the sake of visualization, cells in contact with the repository walls are marked up with spheres if the inflow exceeded two specified thresholds, 0.1 and 0.5 L/min.

The following two features in **Figure 14** are worth noting:

- The ramp seems to have concentrated inflows in its upper part. A part of the simulated inflows to the ramp may be associated with the intersection with the modelled sheet joints which have a very high transmissivity. Note also that transport tunnels and ventilation shafts are open.
- Large inflows at repository depth during operation stage C are predominantly encountered along two lines. This can be explained by the permeability distribution (**Figure 13**).

## 8. Discussion

In the introduction it was argued that the computational grid employed by DarcyTools is a strong feature of the code. In this section this point will be elaborated by an illustration of the cell removal feature. Due to the sparsely fractured rock, many computational cells are not in contact with a fracture and these cells may in many cases be removed; often 70% of the cells can be removed. Without increasing the total simulation time, one can then improve the resolution in other areas.

**Figures 15-17** show a grid for the Forsmark repository, where cells not crossed by a fracture have been removed and the resolution close to deposition holes have been increased. **Figure 15** should be compared with **Figure 10**. White areas in **Figure 15** represent areas where grid cells have been removed. **Figure 16** gives a clearer view of how cells are refined close to deposition tunnels. The smallest cell size in the grid is 0.5 m, which resolves inflows to deposition holes with good resolution, see **Figure 17**. It should be noted that these small cells are part of a computational domain of about  $10 \times 10 \times 1$  km<sup>3</sup> (**Figure 9**) in a seamless way.

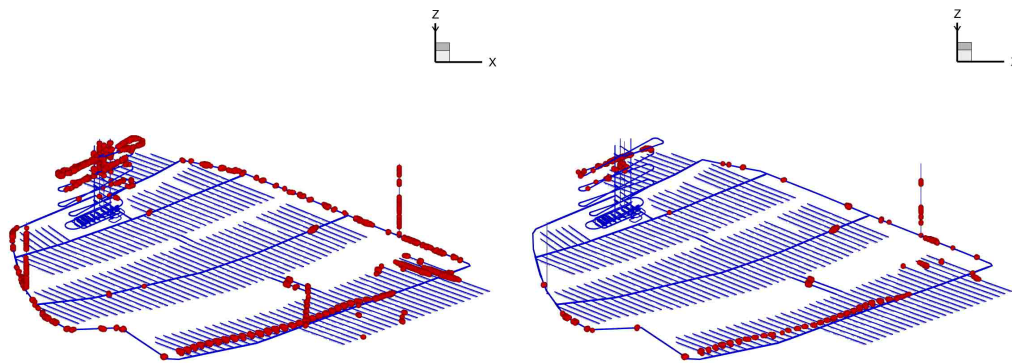


**Figure 14.** Cells with an inflow rate greater than 0.1 L/min (top) and 0.5 L/min (bottom) are marked up by spheres. Operating stage C and grouting level II.

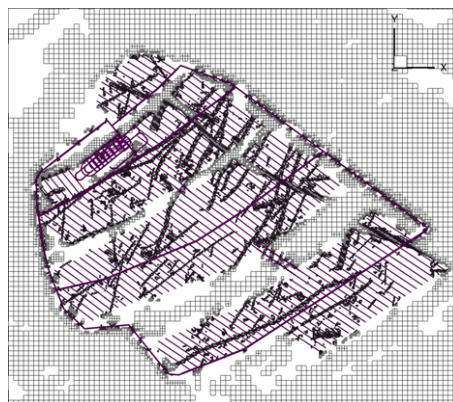


**Figure 15.** Computational grid for the site scale at -465 m elevation.

**Table 4.** Calculated inflow rates (L/s) to different parts of a final repository at Forsmark for three levels of grouting efficiency, I-III, and three stages of operation, A-C. The three operation stages were run in sequence, where stage A lasted for 15 years, stage B lasted for 15 years and stage C lasted for 20 years. CA = central area, DA = deposition area, MT = transportation and main tunnels and VS = ventilation shaft.

Part of repository	Grouting level I			Grouting level II			Grouting level III		
	Operation stage			Operation stage			Operation stage		
	A	B	C	A	B	C	A	B	C
CA-part 1	1	1	2	1	1	1	0	0	0
CA-part 2	0	0	0	0	0	0	0	0	0
CA-part 3	3	3	3	1	1	1	1	1	1
CA-part 4	0	0	0	0	0	0	0	0	0
DA	6	–	–	4	–	–	3	–	–
	–	8	–	–	6	–	–	3	–
	–	–	9	–	–	8	–	–	4
RAMP-part 1	13	14	14	5	5	5	2	2	2
RAMP-part 2	3	3	3	1	1	1	0	0	0
MT	6	6	7	4	4	5	2	2	2
	–	1	1	–	1	1	–	0	0
	–	–	9	–	–	5	–	–	2
VS1	1	1	1	1	1	0	0	0	0
VS2	–	2	2	–	1	1	–	0	0
<b>Total</b>	<b>33</b>	<b>39</b>	<b>51</b>	<b>17</b>	<b>21</b>	<b>28</b>	<b>8</b>	<b>8</b>	<b>11</b>

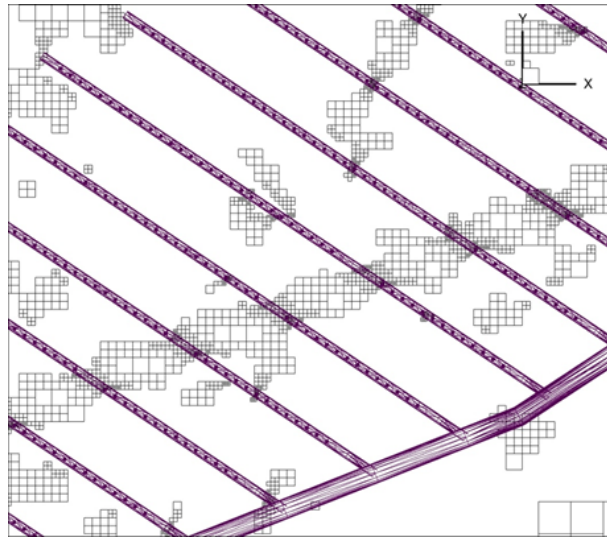


**Figure 16.** Computational grid for deposition tunnel scale. Also the CAD grid for the repository is shown, for orientation.

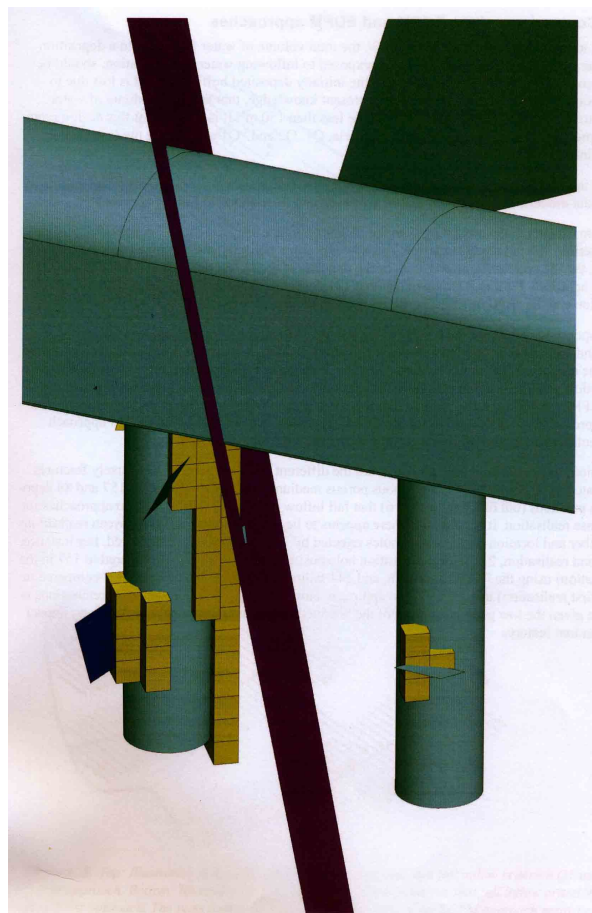


**Figure 17.** Illustration of computational cells in contact with two deposition holes. Also the centre plane of some fractures are shown. The thickness of all fractures was here set to one metre and the computational cells shown are for this reason in contact with the fractures shown.

The solvers, described in Section 5, are developed to handle these kinds of grids in an efficient manner; including the SPMD parallelization.

## 9. Concluding Remarks

A computer code can be designed in various ways, depending on the intended use and the intended user. A code that has a single well defined task will normally put less demand on the user. On the other hand, a code that allows for new equations to be introduced, complex boundary conditions, new source terms, etc will require a deeper understanding from the user. DarcyTools belongs to the latter category. A user should be able to solve a wide range of problems (1D, 2D and 3D, steady/transient, from  $\mu\text{m}$  to km, any kind of boundary condition, arbitrary number of advection/diffusion equations, density stratification, fractured or porous media and more). For this reason, DarcyTools is more of an equation solver than a specific problem solver.

Development is, generally speaking, governed by the demands from applications (see **Table 2**). This development started about 12 years ago and features have been introduced successively since then. Presently developments follow two parallel lines:

- The present version is considered to fulfil most of the demands from the present range of applications. Development is hence directed towards refinement, efficiency and confidence building.
- The next major release will introduce a Navier-Stokes solver. One example of a possible application is flow and transport in a single rock fracture. Such a model can be used to study dispersion at a fracture crossing or for simulating the grouting process. Also turbulent flows (Reynolds equation and advanced turbulence models) will be within scope. Flow beneath an ice sheet is one application in mind, another flow and transport in lakes and rivers (coupled with the groundwater flow).

In addition to the demands from applications, a computer code needs to be continuously developed to make best use of the computer hardware, new solver techniques and developments in programming.

## Acknowledgements

The authors are grateful to the Swedish Nuclear Fuel and Waste Management Company (SKB) for supporting the writing of the paper. Also the free use of DarcyTools, owned by SKB, is acknowledged.

## References

- [1] Jackson, C.P., Andrew, R.H. and Todman, S. (2000) Self-Consistency of Heterogeneous Continuum Porous Medium Representation of a Fractured Medium. *Water Resources Research*, **36**, 189-202.  
<http://dx.doi.org/10.1029/1999WR900249>
- [2] Sahimi, M. (1995) Flow and Transport in Porous Media and Fractured Rock: From Classical Methods to Modern Approaches. VCH., Weinheim, 482pp.
- [3] Hartley, L. and Joyce, S. (2013) Approaches and Algorithms for Groundwater Flow Modeling in Support of Site Investigations and Safety Assessment of the Forsmark Site, Sweden. *Journal of Hydrology*.
- [4] Svensson, U., Ferry, M. and Kuylenstierna, H.-O. (2010) DarcyTools, Version 3.4. Concepts, Methods and Equations. SKB R-10-70, Svensk Kärnbränslehantering AB. 144pp.
- [5] Svensson, U. and Ferry, M. (2010) DarcyTools, Version 3.4. User's Guide. SKB R-10-72, Svensk Kärnbränslehantering AB.
- [6] Svensson, U. (2010) DarcyTools, Version 3.4. Verification, Validation and Demonstration. 2010, SKB R-10-71, Svensk Kärnbränslehantering AB.
- [7] Pruess, K. (1991) TOUGH2 a General-Purpose Numerical Simulator for Multiphase Fluid and Heat Flow. Report, LBNL-29400, Lawrence Berkeley Laboratory, Berkeley, Ca.
- [8] McDonald, M.G. and Harbaugh, A.W. (1988) A Modular Three-Dimensional Finite-Difference Ground-Water Flow Model. 1988, U.S. Geol. Surv. Tech. Water Resour. Invest. Book 6, Chap. 2.
- [9] Hammond, G.E. and Lichtner, P.C. (2010) Field-Scale Model for the Natural Attenuation of Uranium at the Hanford Area Using High-Performance Computing. *Water Resources Research*, **46**, WO9527.  
<http://dx.doi.org/10.1029/2009WR008819>
- [10] Dershowitz, W., Lee, G., Geier, J., Foxford, T. and Ahlstrom, E. (1999) FracMan Interactive Discrete Feature Data Analysis, Geometric Modeling, and Exploration Simulation. User Documentation, Version 2.6, Golder Associates Inc.

- [11] Bian, H.B., Jia, Y., Amand, G., Duveau, G. and Shao, J.F. (2012) 3D Numerical Modeling Thermo-Hydromechanical Behavior of Underground Storages in Clay Rock. *Tunnelling and Underground Space Technology*, **30**, 93-109. <http://dx.doi.org/10.1016/j.tust.2012.02.011>
- [12] Haggerty, R. and Gorelick, S.M. (1995) Multiple-Rate Mass Transfer for Modeling Diffusion and Surface Reaction in Media with Pore-Scale Heterogeneity. *Water Resources Research*, **31**, 2383-2400. <http://dx.doi.org/10.1029/95WR10583>
- [13] Svensson, U. (2001) A Continuum Representation of Fracture Networks. Part I: Method and Basic Test Cases. *Journal of Hydrology*, **250**, 170-186. [http://dx.doi.org/10.1016/S0022-1694\(01\)00435-8](http://dx.doi.org/10.1016/S0022-1694(01)00435-8)
- [14] Svensson, U. (2001) A Continuum Representation of Fracture Networks. Part II: Application to the Äspö Hard Rock Laboratory. *Journal of Hydrology*, **250**, 187-205. [http://dx.doi.org/10.1016/S0022-1694\(01\)00436-X](http://dx.doi.org/10.1016/S0022-1694(01)00436-X)
- [15] Diskin, B., Thomas, J.L., Nielsen, E.J., Nishikawa, H. and White, J.A. (2010) Comparison of Node-Centered and Cell-Centered Unstructured Finite-Volume Discretizations: Viscous Fluxes. *American Institute of Aeronautics and Astronautics*, 48.
- [16] Spalding, D.B. (1972) A Novel Finite Difference Formulation for Differential Expressions Involving Both First and Second Derivatives. *International Journal for Numerical Methods in Engineering*, **4**, 551-559. <http://dx.doi.org/10.1002/nme.1620040409>
- [17] Roache, P.J. (1976) Computational Fluid Dynamics. Hermosa Publs., Albuquerque, 446pp.
- [18] Aftosmis, M.J., Berger, M.J. and Melton, J.E. (1999) Adaptive Cartesian Mesh Generation. In: Thompson, J.F., Soni, B.K. and Weatherill, N.P., Eds., *Handbook of Grid Generation*, CRC Press, Boca Raton, 1136pp.
- [19] Saad, Y. and Schultz, M.H. (1996) GMRES: A Generalized Minimal Residual Algorithm for Solving Nonsymmetric Linear Systems. *SIAM Journal of Scientific and Statistical Computing*, **7**, 856-869.
- [20] Stüben, K. and Trottenberg, U. (1982) Multigrid Methods: Fundamental Algorithms, Model Problem Analysis and Applications. *Multigrid Methods, Lecture Notes in Mathematics*, **960**, 176.
- [21] Stüben, K. (2001) Algebraic Multigrid (AMG): An Introduction with Applications. In: Trottenberg, U., Oosterlee, C. and Schüller, A., Eds., *Multigrid*, Academic Press, London.
- [22] Ferry, M. (2002) New Features of MIGAL Solver. *9th International PHOENICS Users Conference*, Moscow.
- [23] Aftosmis, M.J., Berger, M.J. and Murman, S.M. (2004) Applications of Space-Filling Curves to Cartesian Methods for CFD. 42nd AIAA, Aerospace Sciences Meeting and Exhibition, Chapter.
- [24] Sagan, H. (1994) Space Filling Curves. Springer-Verlag, 193pp. <http://dx.doi.org/10.1007/978-1-4612-0871-6>
- [25] Selroos, J-O. and Follin, S. (2010) SR-Site Groundwater Flow Modeling Methodology, Setup and Results. SKB R-09-22, Svensk Kärnbränslehantering AB. 125pp.
- [26] Vidstrand, P., Follin, S. and Zugec, N. (2010) Groundwater Flow Modeling of Periods with Periglacial and Glacial Climate Conditions—Forsmark. SKB R-09-21, 190pp, Svensk Kärnbränslehantering AB.
- [27] Svensson, U. and Follin, S. (2010) Groundwater Flow Modelling of the Excavation and Operational Phases—Forsmark. SKB R-09-19, Svensk Kärnbränslehantering AB.
- [28] Joyce, S., Applegate, D., Hartley, L., Hoek, J., Simpson, T., Swan, D. and Marsic, N. (2010) Groundwater Flow Modelling of Periods with Temperate Climate Conditions—SR-Site Forsmark. SKB R-09-20, 2010, Svensk Kärnbränslehantering AB.